AN AQUEOUS LITHIUM BROMIDE ABSORPTION REFRIGERATOR
Part II experimental investigation

Satha Aphornratana

Department of Mechanical Engineering

Sirindhorn International Institue of Technology

Thammasat University

P.O.Box 22 Thammasat Rangsit Post Office,

Patumthani 12121, Thailand

Tel. (662) 5164357-8 Ext. 2208 Fax. (662) 5164359

SUMMARY

In this paper, an absorption refrigerator using lithium bromide-water as the working fluid was investigated experimentally. A small scale experimental unit was designed and built. It was used to study the system performance at various operating conditions. It was tested with the generator temperature ranging from 65 to 85°C, evaporator temperature ranging from 3 to 11°C, and absorber and condenser temperatures ranging from 25 to 45°C. The effects of the heat exchanger effectiveness and the solution circulation rate on the system performance were also studied. The experimental results were also compared with theoretical data.

1. INTRODUCTION

This paper is the second part of a two paper series. In the first part, [Aphornratana, 1995], an absorption refrigeration cycle using aqueous lithium bromide as the working fluid was studied theoretically. Solution Circulation Ratio (SCR) was found to have a strong effect on the system performance; the lower the SCR, the higher the Coefficient of Performance (COP). This is because an increase in SCR requires more heat input at the generator. To overcome this problem, a solution heat exchanger should be employed.

In this part, an absorption refrigerator using lithium bromide-water as the working fluid was investigated experimen-

tally. A small scale experimental unit was designed and built. It was used to study the system performance at various operating conditions. It was tested with the generator temperature ranging from 65 to 85°C, evaporator temperature ranging from 3 to 11°C, and absorber and condenser temperatures ranging from 25 to 45°C. The effects of the heat exchanger effectiveness and the solution circulation rate on the system performance were also studied. The experimental results were also compared with the theoretical data based on the model developed in part I.

2. EXPERIMENTAL REFRIGERATOR

An experimental refrigerator with a cooling capacity of 2 kW was constructed. Figure 1 shows a schematic diagram of the system. All vessels were constructed from stainless steel. Copper and nylon tubes with brass fittings were used for water and steam while stainless steel and nylon tubes with stainless steel fittings were used with the lithium bromide solution.

The generator design was based on the thermosiphon principle with baffle plates located at its upper end to prevent liquid droplets being carried over with the refrigerant vapour. The maximum heating capacity of the generator was 7 kW, provided by two 3.5 kW heaters. The evaporator design was based on a flash-evaporation principle. A single 3.5 kW electric heater located within the evaporator vessel was used to provide a cooling load. The output of all electric heaters was controlled using variable transformers. The condenser was a shell and coil type cooled by water taken from the laboratory's cooling tower. An absorber used was based on falling film column. Its consisted of an internal vertical cooling coil with lithium bromide solution sprayed on the top coil to create a liquid film. The solution heat exchanger consisted of seven double pipe heat exchangers connected in series. The hot solution from the generator and the cold solution from the absorber flowed counter currently through the annular duct and inner tube respectively. Twisted tapes were inserted into the inner tube to improve the heat transfer coefficient by creating turbulent mixing.

Four circulation pumps were used; one to circulate water through the flash type evaporator, another to circulate lithium bromide solution through the absorber, another to pump the solution from the absorber to the generator, and the fourth to pump water from the condenser to the evaporator and to the generator when the system is shut down.

The experimental refrigerator was designed to be computer controlled. Maximum electrical power inputs to the generator and evaporator heaters were set using variable transformers, however, fine

adjusting of these inputs was achieved by on-off switching via electrical relays, controlled automatically through a computer to maintain selected set-point temperatures. Power supplied to the heaters were measured using voltage and current transducers and recorded automatically by the computer. Condenser and absorber temperatures were controlled by varying cooling water flow rates using proprietary solenoid control valves. Sight glasses were provided in each vessel to allow liquid levels to be monitored. Liquid levels were controlled through infra-red switches positioned on the sight glasses. In each case a small plastic float interrupted an infra-red beam, as the liquid level rose above or fell below the set point level, causing an electrical signal to trigger the opening or closing of a solenoid valve in the liquid feed pump circuit.

The evaporator and condenser were charged with deionized water. The generator and absorber were charged with lithium bromide solution with mass concentration of 54% and included a proprietary corrosion inhibitor.

The performance of the experimental refrigerator was obtained by measuring the time averaged electric power input to the evaporator and generator heaters over a steady state running time of 30 to 60 minutes. Results over a range of operating temperatures and pressures at the generator, absorber, condenser, and evaporator were recorded.

3. EXPERIMENTAL METHOD

Even though all the system was designed to be fully automatically controlled, the examples of the operating techniques are provided by assuming that the system is manually operated and controlled.

Before operating the system, all non-condensable gases must be removed from the system. A vacuum pump is used to evacuate the system for 5 to 10 min. When all the gases are removed, the pressure measured by a digital manometer installed at the condenser shows a minimum value.

At first, all the solution collected in the absorber is transferred to the generator using the solution pump (5), then the generator heaters are switched on. As the water continues to boil out from the solution, without any cooling water flowing through the condenser coils, the pressures in the generator and condenser contiue to rise. When the required pressure is attained, the cooling water is turned on to a flow rate such that a steady pressure can be maintained. After 15 to 20 min, the solution concentration in the generator is increased to a sufficient value, Having obtained the desired temperature and pressure of the solution in the generator, valve (3) is opened to allow the concen-

trated solution to feed the absorber. The flow rate is then adjusted to a desired value (indicated by the flow meter). After sufficient solution collects at the bottom of the absorber, the recirculation pump (4) and the solution pump (5) are switched on. The flow rate of the solution being pumped is adjusted (using valve 6, valve 7 is initially off) so that a constant level in the absorber is maintained. At this stage, the solution is pumped directly to the generator without passing through the solution heat exchanger. When the required absorber temperature is attained, turn on the cooling water and the evaporator recirculation pump (2). Adjust the cooling water flow rate in order to maintain a constant temperature in the absorber. As the evaporator temperature continues to drop, the heater is turned on. The heater power input is gently adjusted in order to maintain a constant temperature. In oreder to improve the system performance, the valves 6 and 7 are carefully adjusted, so that a desired temperature of the concentrated solution at the flow meter inlet is attained. This temperature must be above the crystallisation value.

When the system is ready to be to be shut down, the following procedures must be followed in order to avoid crystallisation. As the solution is collected in the generator, solution heat exchanger, and pipe lines, there is a concentration range from 60 to 65%. For such high concentration, if the solution cools down to the ambient temperature, it will crystallise. Thus, it must be diluted to a concentration sufficiently below the crystallisation limit at the ambient temperature. After all the heaters are switched off, the condensate collected in the condenser can be pumped (through pump 8) into the solution heat exchanger and the generator through valve 9, and into the absorber through valve 10.

4. PARAMETERS USED IN THE ANALYSIS

Theoretical values of Coefficient of Performance (COP_{theo}) and Solution Circulation Ratio (SCR_{theo}) were obtained from the method provided in part I, [Aphornratana 1995]. In order to enable a true comparison between theoretical and experimental values, a pressure drop of 3 mbar was assumed between the generator and condenser, and a pressure drop of 2 mbar was assumed between the evaporator and absorber. These pressure losses were estimated using standard methods, [Streeter & Wylie 1975].

Experimental Coefficient of Performance values, based on the electric power input to the generator and evaporator were used here. These, however, included unwanted heat losses and gains, therefore:

$$COP_{elce} = \frac{evaporator\ heat\ input}{generator\ heat\ input} \qquad (1)$$

Experimental Solution Circulation Ratio values (SCR_{exp}) were obtained by

measuring the evaporation rate of the refrigerant in the evaporator and the solution circulation rate between the absorber and the generator using a flow meter located between the flow control valve and the absorber. Refrigerant mass flow rates were obtained by measuring the changes in liquid volume of the evaporator over a finite time (flow meter can not be used as the flowrate is very small and not continuous).

The elimination of all unwanted heat losses and gains will lead to obtain a truer indication. In order to achieve this aim and to make a comparison between the theoretical prediction and experimental results, generator and evaporator heat inputs were calculated using the measured mass flows and thermodynamic properties of the working fluids. The fluid properties were obtained from the correlations of Patterson & Perez-Blanceo [1988] and a standard steam properties table, using measured values of pressures and temperatures. The generator power input was obtained by considering the generator and the solution heat exchanger as a single control volume (Figure 2), therefore:

$$\dot{Q}_{gen,\ mass} = \dot{m}_5 \cdot h_5 + \dot{m}_4 \cdot h_4 - \dot{m}_3 \cdot h_3 \quad (2)$$

The evaporator power input was obtained from:

$$\dot{Q}_{evap,\ mass} = \dot{m}_1 \cdot (h_1 - h_2) \quad (3)$$

The COP based on the mass flow rate was obtianed from:

$$COP_{mass} = \frac{\dot{Q}_{evap,\ mass}}{\dot{Q}_{gen,\ mass}} \quad (4)$$

5. EXPERIMENTAL RESULTS AND DISCUSSIONS

The system was tested over a range of operating temperatures. The flow rate of the concentrated solution, returning back to the absorber from the generator, was adjusted to half of the flow meter full scale. However, as the density and viscosity of the solution varied with temperature and concentration, the mass flow rate ranged from 0.82 to 1.05 kg/min. Solution concentration was calculated from the generator temperature and pressure, assuming equilibrium state. The temperature of the concentrated solution, leaving the solution heat exchanger was normally adjusted to 50°C. This caused the solution heat exchanger effectiveness to range between 0.4 to 0.8. Figures 3 to 10 show plots of the experimental and theoretical performance of the system over the range of operating temperatures.

COP_{elec} was found to be approximately 75% of COP_{mass}. The combined average heat loss from the generator and the solution heat exchanger was estimated to be approximately 20% of the electric power input to the generator. The average unwanted heat gains to the evaporator were found to

be approximately 5% of the electric power input. Even when all the unwanted heat transfers were eliminated from the calculation, the COP_{mass} was found to be around 80% of the theoretical value (COP_{theo}). The difference was thought to be resulted from the unexpectedly high SCR_{exp}. This was found to be around 2 to 5 times greater than the theoretical prediction. The difference between SCR_{exp} and SCR_{theo} reduced when cooling capacity decreased. The difference between SCR_{exp} and SCR_{theo} can be explained as follows; at higher cooling capacities, greater absorption rates are required, and for the same mass transfer area (the absorber coil surface), the solution concentration in the absorber was increased to increase the mass fransfer capacity. This results in a non-equilibrium state of solution in the absorber and a high SCR_{exp}. Referring to Figure 2, an absorber effectiveness may be defined as a ratio between actual and theoretical concentration change in the absorber [George & Murthy 1989], therefore;

$$\varepsilon_{abs} = \frac{X_4 - X_{3,\,exp}}{X_4 - X_{3,\,theo}} \qquad (5)$$

Four thermocouple probes were installed at the generator. The tests showed that, the temperatures of liquid and vapor were within $\pm 2^{\circ}C$. Thus, a good mixing of the solution during the boiling process was achieved. It was, therefore, reasonable to assume that, solution was in an equilibrium state at its temperature and pressure. The actual concentration of solution in the absorber may be obtained by assuming that solution in the generator was in equilibrium state, and the actual SCR_{exp} was already measured, thererfore;

$$X_{3,exp} = X_4\ (1\text{-}1/SCR_{exp}) \qquad (6)$$

For the absorber used, the effectiveness was found to be between 0.2 to 0.5. An increase of cooling capacity (or an increase of absorption rate) by increasing the solution circulation rate reduced the absorber effectiveness. It can be seen from Figures 11 and 12 that SCR_{exp} was increased while both COP_{mass} and COP_{elec} were decreased when increasing the cooling capacity by increasing the solution circulation rate. In theory, for given operating temperatures, cooling capacity increases linearly with the solution circulation rate and both SCR_{theo} and COP_{theo} are independent of the solution circulation rate.

The surface area of the absorber cooling coil was nearly twice that of the calculated value. However, it is not possible to say that the coil surface was completely wetted. Before being fitted in the absorber shell, the coil was tested with a water shower. This showed that the wetted area was in fact less than half of the total surface area. In order to create a good liquid film, some kind of treated surface or high recirculation rate is required. [Carey 1984].

During the experiments, it was found that the absorber performance was improved significantly if the solution recirculation rate through the spray head was increased by changing the recirculation pump capacity from 20 to 90 W.

Figures 13 and 14 show the variation of system performance with the solution temperature measured at the absorber inlet. This reflects the changes in the solution heat exchanger effectiveness. For given operating temperatures and solution circulation rates, the solution bypass valve was adjusted to give the required temperature. Figures 13 and 14 show that SCR_{exp} and cooling capacity were independent of solution heat exchanger effectiveness. The COP_{mass} and COP_{elec} were found to increase when the temperature of the concentrated solution entering the absorber was reduced (increasing the solution heat exchanger effectiveness). These experiments showed that the use of a solution heat exchanger could reduce the power input to the generator by up to 60%, and increased COP as a result. As the SCR_{exp} was higher than the SCR_{theo}, the effect of the solution heat exchanger on improving COP was more important than expected from the theoretical prediction.

6. CONCLUSION

Experimental studies of the single-effect absorption refrigerator using aqueous lithium bromide were described. The system was tested with various operating temperatures, solution circulation rates, and heat exchanger effectiveness. A Coefficient of Performance based on electric power input to the evaporator and generator (COP_{elec}) of 0.4 to 0.6 was found. When all unwanted heat transferred was eliminated from the performance calculation, a Coefficient of Performance based on working fluid mass flows and thermodynamic properties (COP_{mass}) of 0.5 to 0.8 was found. The COP of the absorption cycle was fairly constant over a wide range of operating temperatures. Experimental performance date were compared with theoretical predictions based on the model described in part I, Aphornratana [1995]. COP_{mass} was found to be approximately 80% of the theoretical value. The difference was thought to result from an unnecessarily high Solution Circulation Ratio (SCR_{exp}), which was 2 to 5 times greater than the theoretical value (depending on the cooling capacity). This was as a result of the low mass transfer performance of the absorber. If a more effective absorber was used, system performance as high as the theoretical prediction should be achieved.

As the experimental Solution Circulation Ratio (SCR_{exp}) was significantly greater than the theoretical predictions, the importance of the solution heat exchanger to the improvement of the cycle

COP was increased. The study indicated that the generator energy input can be reduced by up to 60% by using a solution heat exchanger and this results in a greater COP. The experiments also showed that the system can be operated with the generator temperature as low as 65 °C and yet still maintain a good degree of performance.

NOMENCLATURES

COP	Coefficient of Performance
h	specific enthalpy ($kJ.kg^{-1}$)
m	mass flow ($kg.sec^{-1}$)
$\dot{Q}$	heat energy rate (kW)
$\dot{S}CR$	Solution Circulation Ratio
X	mass concentration

SUBSCRIPTS

1, 2, 3,...	see relevant figures
abs	absorber
evap	evaporator
exp	experimental data
elec	date based on electrical power input
gen	generator
mass	data based on mass flow of the working fluids
theo	theoretical data

REFERENCES

Aphornratana, A. (1995), "An aqueous lithium bromide absorption refrigerator : Part I theoretical investigation", Research and Development Journal of The Engineering Institute of Thailand, Vol. 6, pp 57-66.

Carey, C.O.B. (1984), "Research and testing of working fluids suitable for an absorption heat pump to heat building", Ph.D. thesis, Cranfield Institute of Technology, U.K..

George, J. M., and Murthy, S.S. (1989), "Influence of absorber effectiveness on performance of vapour absorption heat transformers", Int. J. Energy Research, Vol. 13, pp 629-638.

Patterson, M. R., and Perez-Blanco, H. (1988), "Numerical fits of properties of lithiumbromide water solution", ASHRAE Trans., Vol. 94, Part 2, pp 2059-2077.

Streeter, V. L., and Wylie, E. B. (1975), "Fluid mechanics$^{6ed.}$ ", McGraw-Hill Book Company, N.Y..

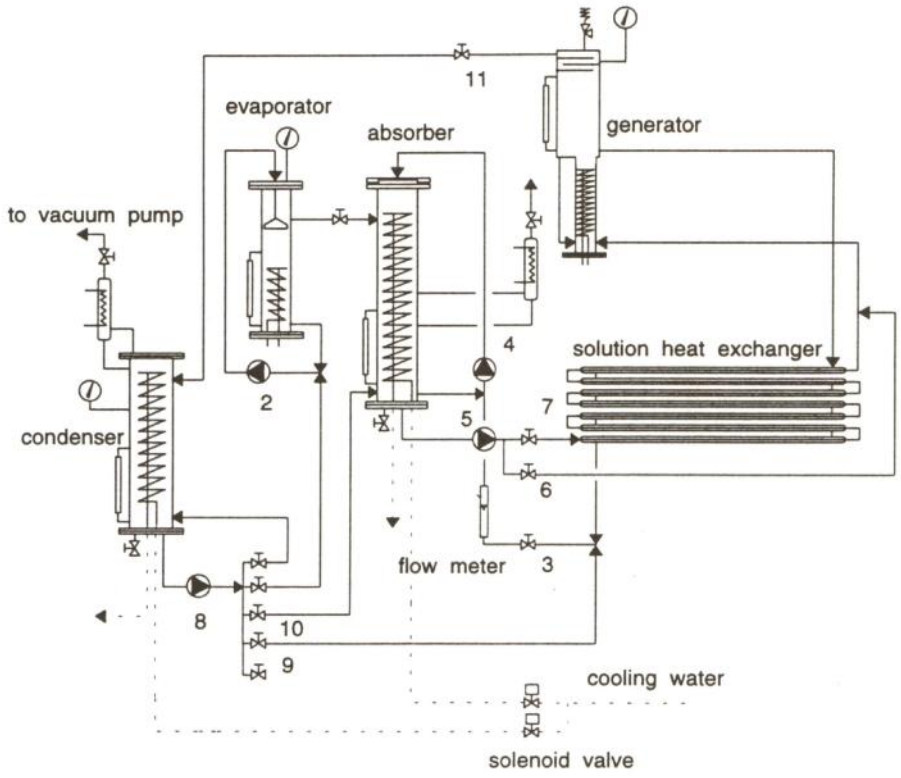

Figure 1 Schematic diagram of the experimental refrigerator.

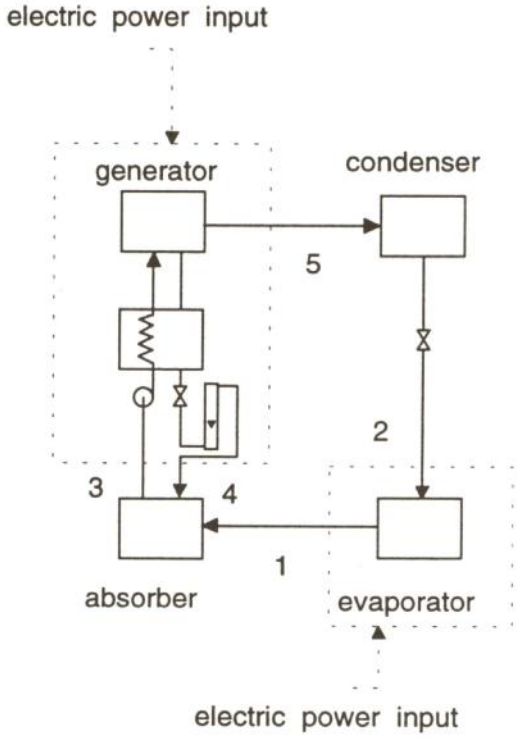

Figure 2 Control volumes used for calculating the performance based on working fluids mass flow.

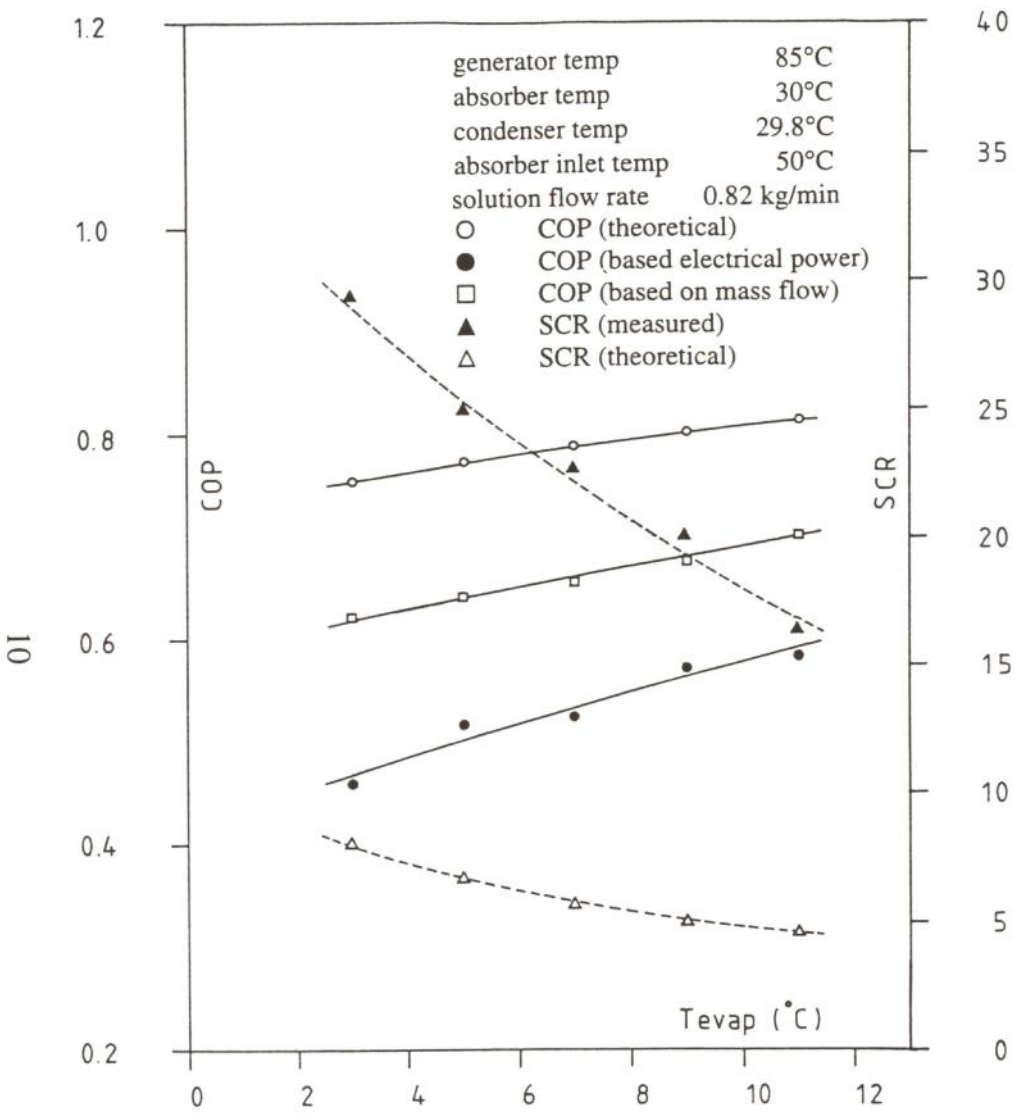

Figure 3 Effect of evaporator temperature on theoretical and experimental COP and SCR.

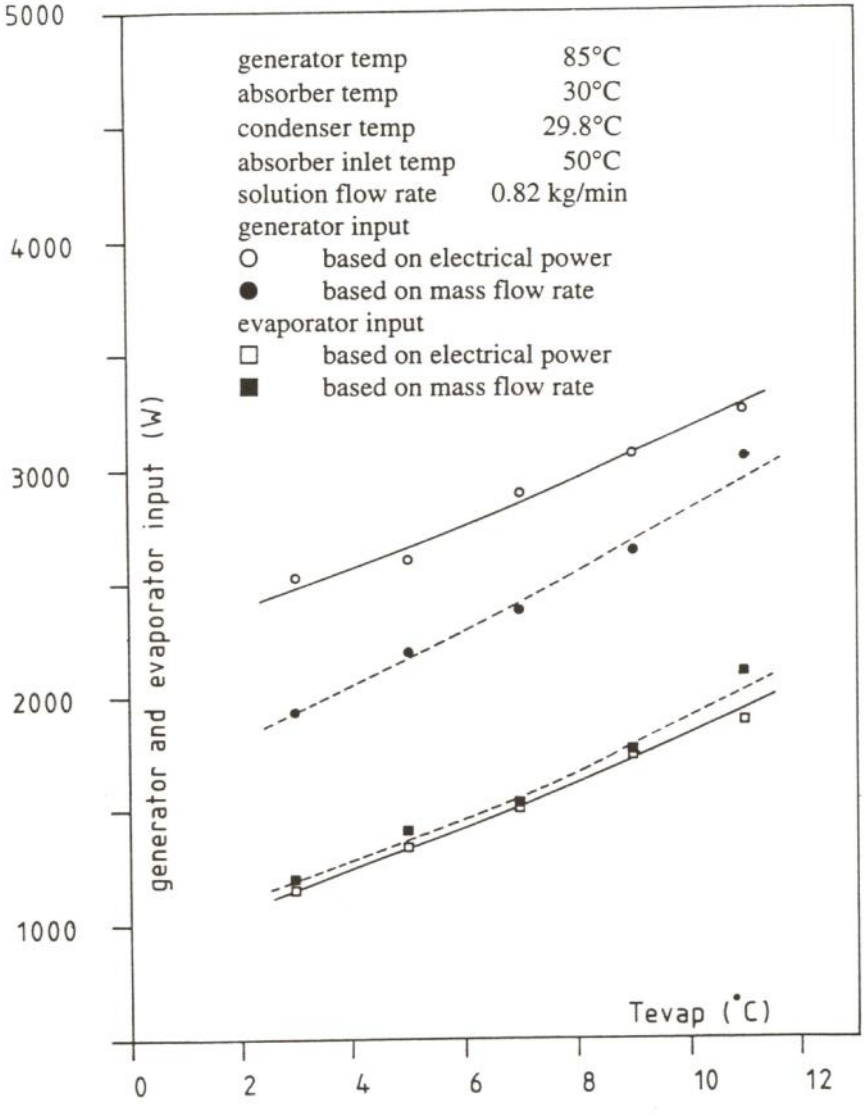

Figure 4 Effect of evaporator temperature on heat input to the evaporator and generator.

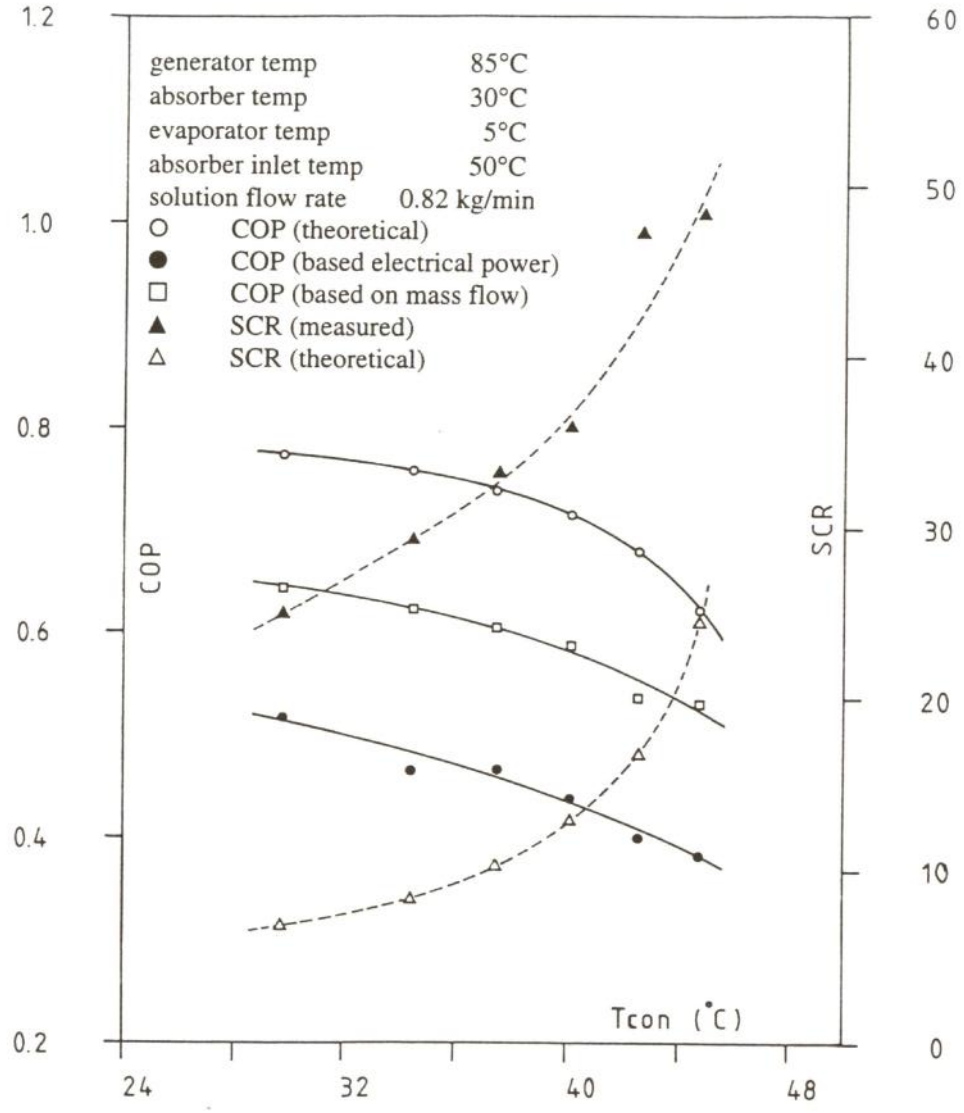

Figure 5 Effect of condenser temperature on theoretical and experimental COP and SCR.

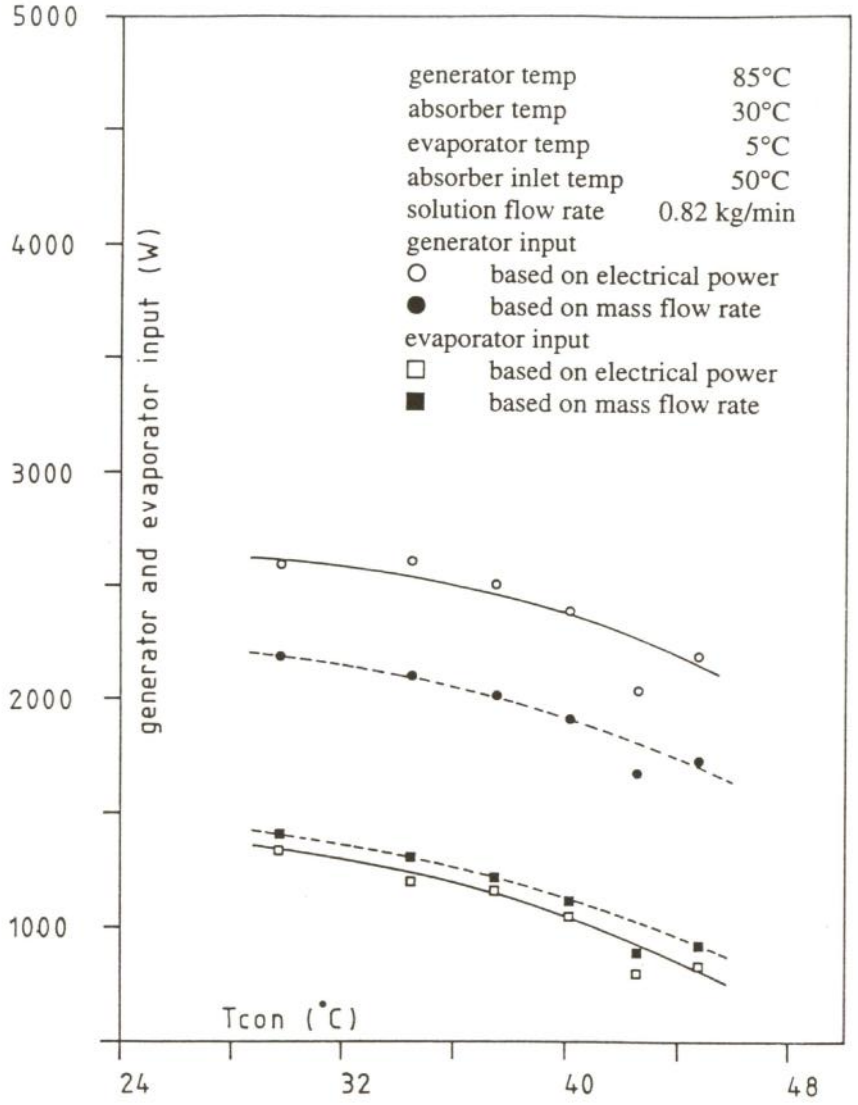

Figure 6 Effect of condenser temperature on heat input to the evaporator and generator.

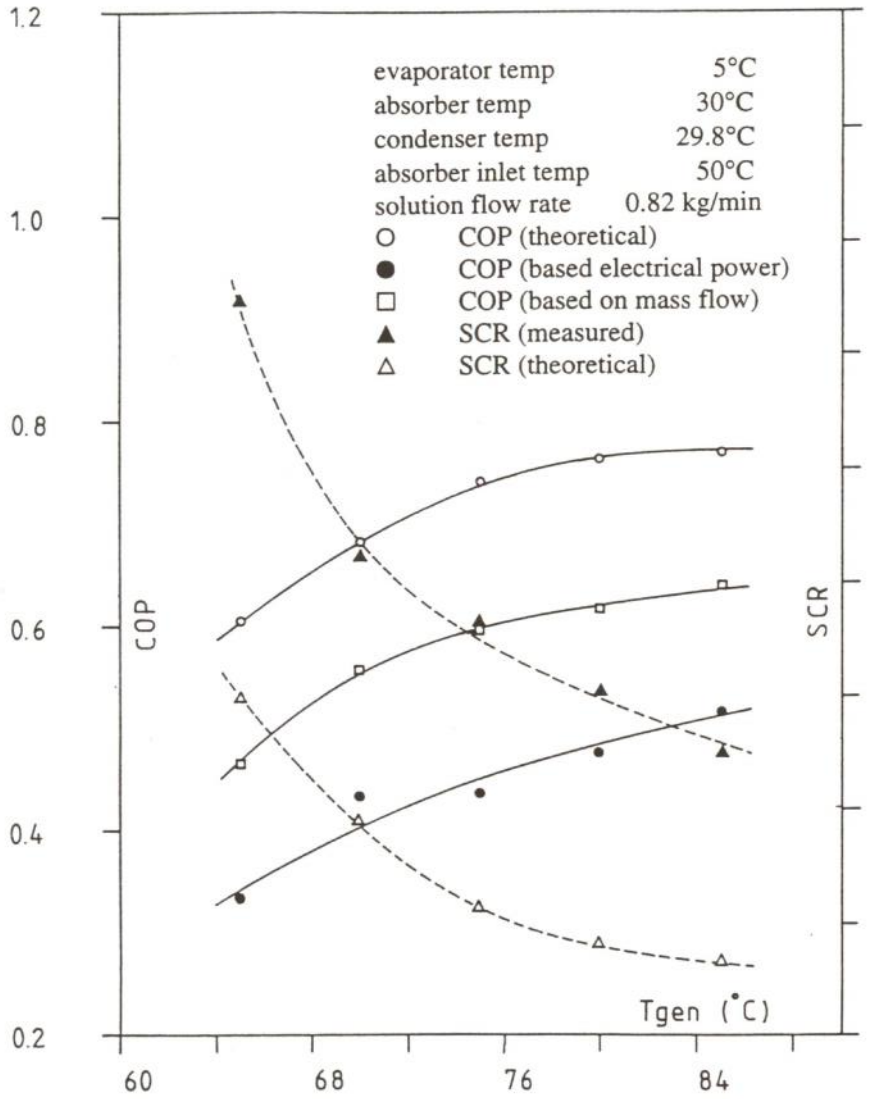

Figure 7 Effect of generator temperature on theoretical and experimental COP and SCR.

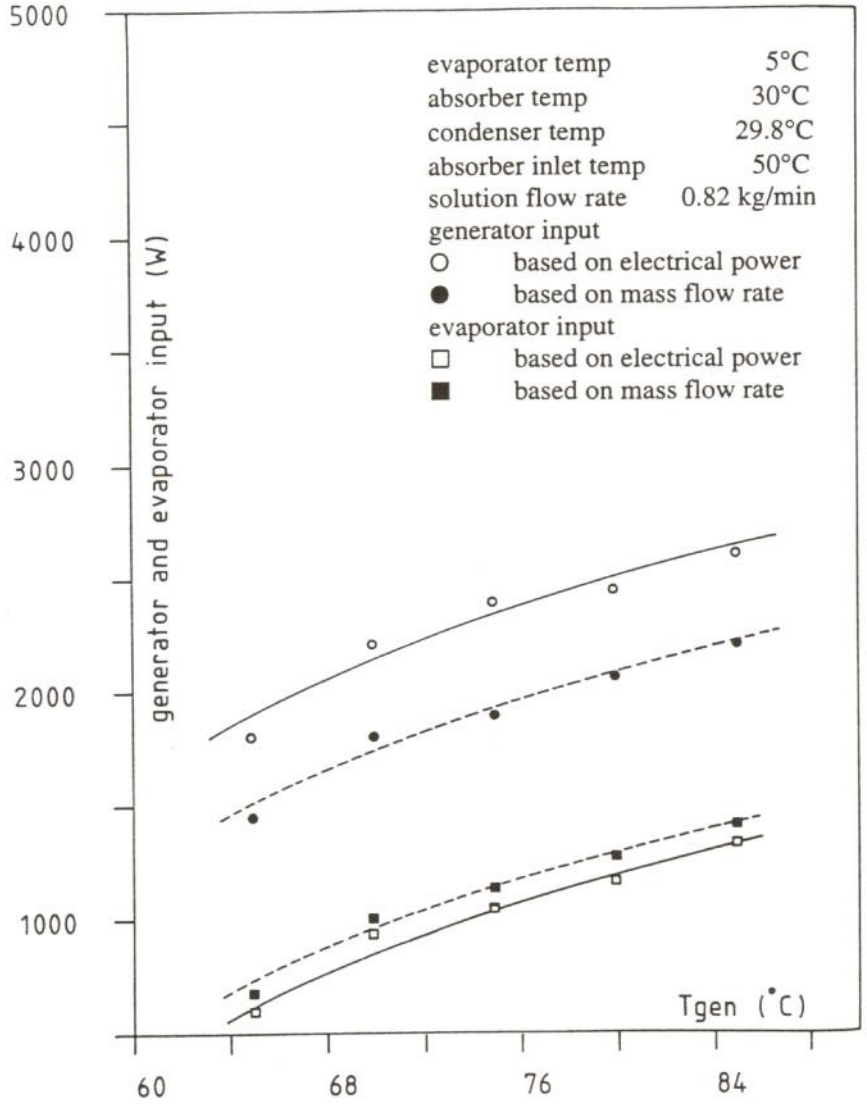

Figure 8 Effect of generator temperature on heat input to the evaporator and generator.

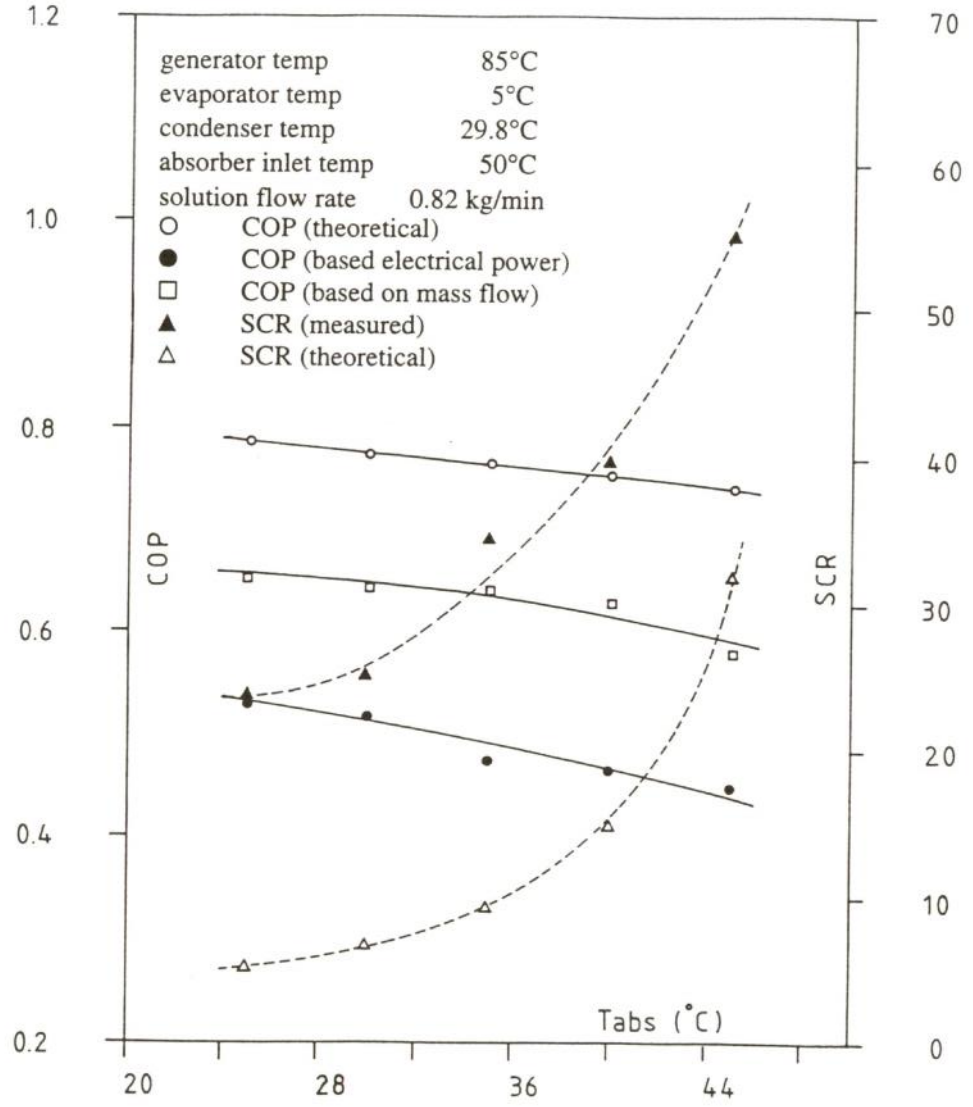

Figure 9 Effect of absorber temperature on theoretical and experimental COP and SCR.

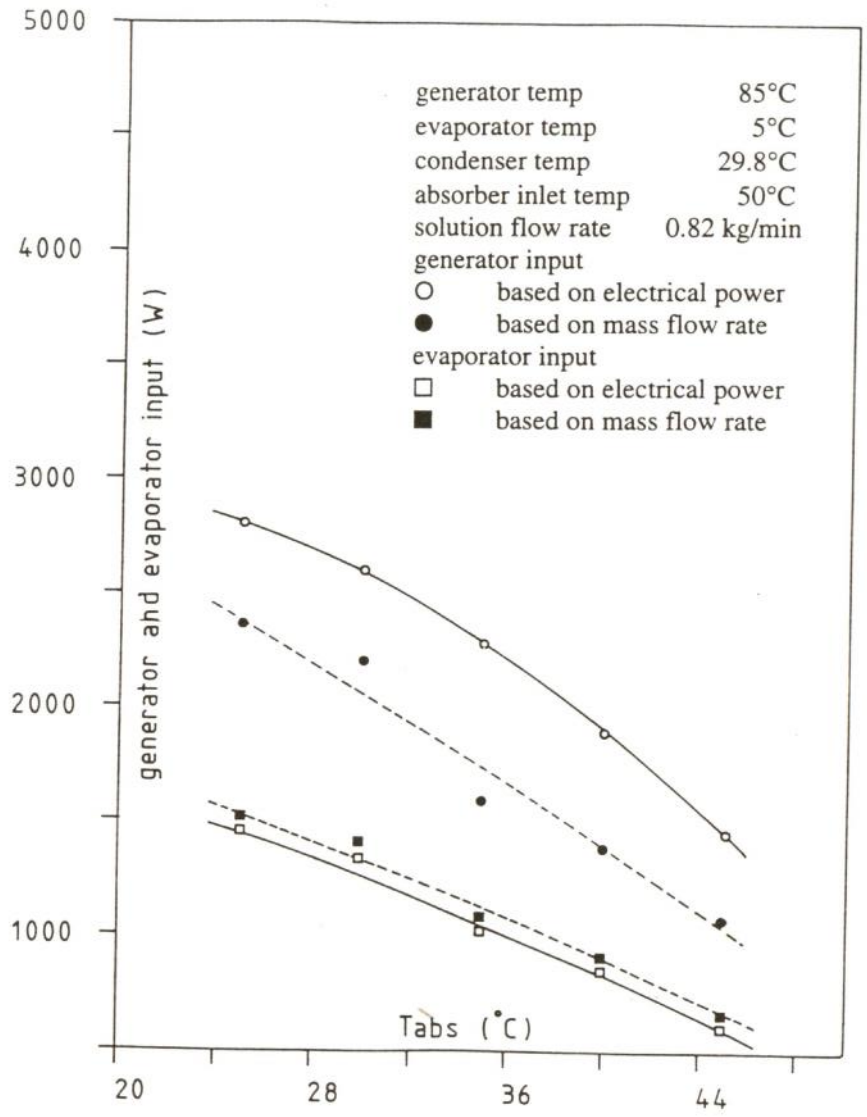

Figure 10 Effect of absorber temperature on heat input to the evaporator and generator.

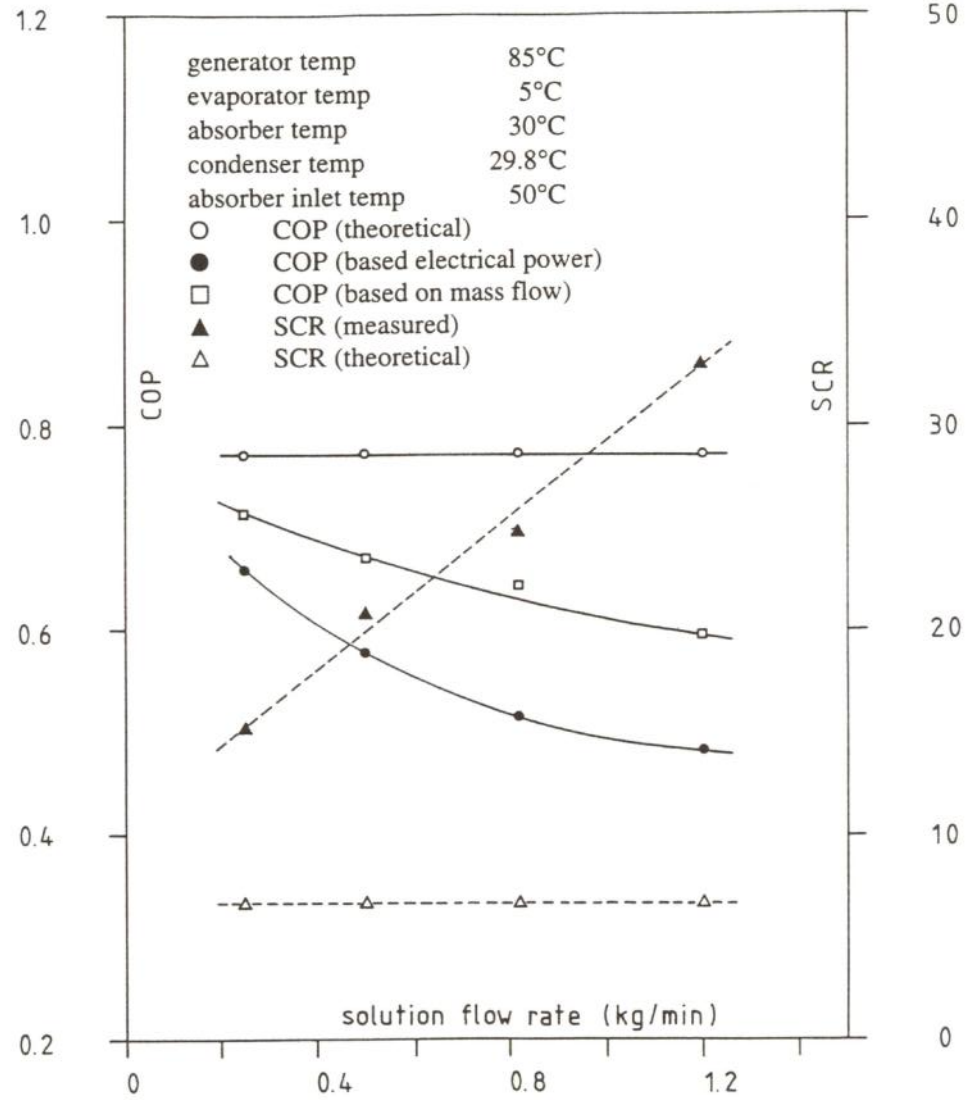

Figure 11 Effect of solution circulation rate on theoretical and experimental COP and SCR.

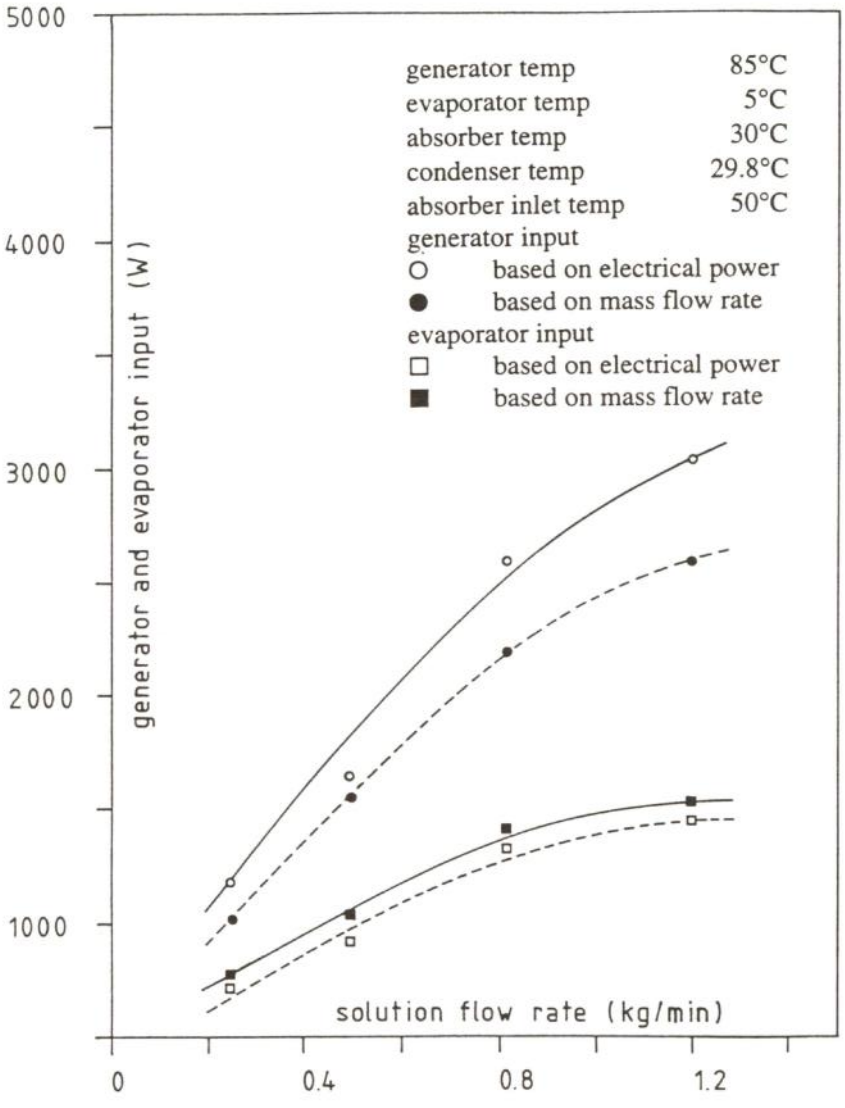

Figure 12 Effect of solution circulation rate on heat input to the evaporator and generator.

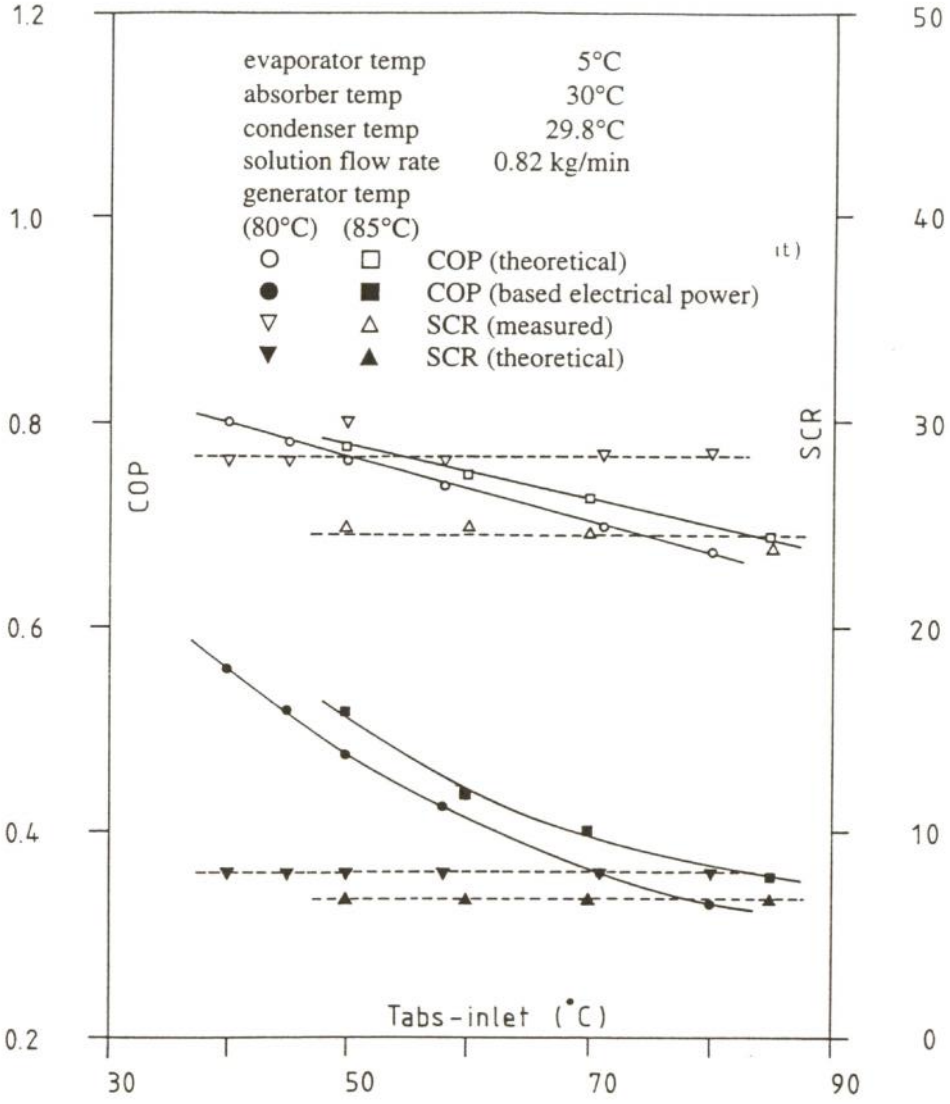

Figure 13 Effect of solution temperature (entering the absorber) on theoretical and experimental COP and SCR.

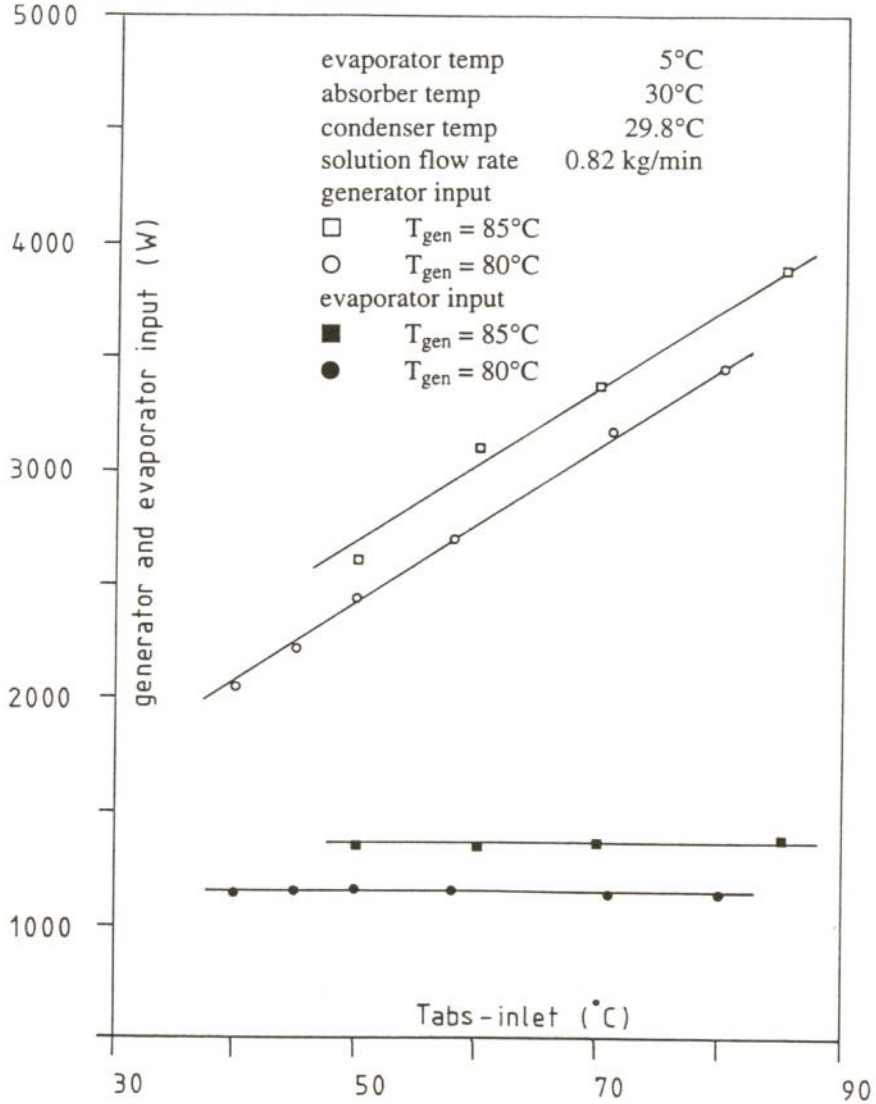

Figure 14 Effect of solution temperature (entering the absorber) on heat input to the generator and evaporator.